Biosensors and Bioelectronics 129 (2019) 58–63

Contents lists available at ScienceDirect

Biosensors and Bioelectronics

journal homepage: www.elsevier.com/locate/bios

Electrochemical aptasensor for aflatoxin B1 based on smart host-guest recognition of β-cyclodextrin polymer

Shuang Shuang Wu[a], Min Wei[a,b,*], Wei Wei[a,*], Yong Liu[c], Songqin Liu[a]

[a] Jiangsu Engineering Laboratory of Smart Carbon-Rich Materials and Device, Jiangsu Province Hi-Tech Key Laboratory for Bio-medical Research, School of Chemistry and Chemical Engineering, Southeast University, Nanjing 211189, China
[b] College of Food Science and Technology, Henan University of Technology, Zhengzhou 450001, China
[c] College of Chemistry and Chemical Engineering, Henan University, Kaifeng 475004, PR China

ARTICLE INFO

Keywords:
Aflatoxin B1
β-cyclodextrin
Host-guest recognition
AC impedance
Differential pulse voltammetry
Electrochemical aptasensor

ABSTRACT

Developing a simple and reliable method for the detection of the highly concerning mycotoxin, aflatoxin B1 (AFB1), is of great importance to food safety monitoring. In this study, a simple electrochemical aptasensor was presented for the detection of AFB1 based on the host-guest recognition between ferrocene and β-cyclodextrin (β-CD). Fc-labeled aptamer of AFB1 first hybridized with its complementary Fc-cDNA. Two ferrocene molecules were brought closely together and couldn't enter into the cavity of β-CD modified on the electrode. Negligible signal could be observed. Once AFB1 captured the aptamer from the AFB1-sensitive dsDNA, Fc-cDNA was released and subsequently entered into the cavity of β-CD to form inclusion complexes, giving rise to an distinct increase of R_{et} and peak current because of the molecular recognition of β-CD. AC impedance method is more sensitive than DPV method. The electrochemical aptasensor displayed a sensitive response to AFB1 in a wide linear range of 0.1 pg/mL to 10 ng/mL, with a low detection limit of 0.049 pg/mL (0.147 pmol/mL) by AC impedance detection, which is 10–100 lower than previously reported methods. The aptasensor has good selectivity and reliability, which has been successfully applied to the determination of AFB1 in real peanut oil samples with recoveries ranging from 94.5% to 106.7% and inter-assay RSD lower than 11.51%.

1. Introduction

As is known to all that toxigenic fungi can produce agricultural commodity contamination mycotoxins (Lin et al., 2015). Aflatoxins are toxic and generally identified as potent carcinogens, mutagens and teratogens. Among the aflatoxin family, aflatoxin B1 has the highest toxicity in known chemical carcinogens owing to its teratogenic, hepato-toxic, carcinogenic and mutagenic adverse effects toward humans (Reddy et al., 2009; Hontanaya et al., 2015). Especially, when the grain crops are stored in hot and humid environment, intermediate medium for genetic toxicity might be produced, which is a great cause of acute cancer, liver damage and liver cirrhosis (Zhao et al., 2017a, 2017b). Thus, taking into account the risks of AFB1, the development of reliable and sensitive analytical methods for the determination of trace AFB1 is essential for food safety. Up to now, many typical instrumental analytical methods have been reported for AFB1 detection, including high performance liquid chromatography (HPLC), liquid chromatography combined with mass spectrometry and thin layer chromatography (Ma et al., 2016a, 2016b; Zhou et al., 2016; Annunziata et al., 2017; Irakli et al., 2017). Although these assays have good sensitivity, they are limited to well-trained operators and expensive instruments.

Aptamers are sequence of single-chain oligonucleotides with high affinity and specific recognition capabilities for the targets via the formation of distinct secondary and specific tertiary structures (Knight et al., 2009; Mayne et al., 2018). They have many applications in bioimaging and therapeutics and as recognition elements in many biosensing platforms, such as protein, toxins, peptides and cells (Gao et al., 2017; Lin et al., 2017; Zhao et al., 2017a, 2017b; Xu et al., 2018). They are isolated from combinatorial oligonucleotide libraries containing 104–1015 different sequences by an in vitro process known as Systematic Evolution of Ligands by EXponential enrichment (SELEX) (Xu et al., 2016; Platt et al., 2009). In addition, aptamers can also be easily functionalized with various fluorescent groups, functional groups, biotins and proteins, simplifying detection processes and making the sensing platform more flexible and multifunctional.

Electrochemical detection, a powerful analytical technique, has been widely applied for the large-scale applications in environmental monitoring and food safety, due to its simple operation, low

* Corresponding authors.
E-mail addresses: wei_min80@163.com (M. Wei), weiw@seu.edu.cn (W. Wei).

https://doi.org/10.1016/j.bios.2019.01.022
Received 20 November 2018; Received in revised form 15 January 2019; Accepted 17 January 2019
Available online 19 January 2019
0956-5663/

background signal, quick response and high sensitivity (Xia et al., 2017). β-cyclodextrin (β-CD), a kind of oligosaccharides with external hydrophilic groups and internal hydrophobic groups, has the property of supramolecular host-guest chemistry. The host-guest molecular recognitions are dependent on their molecular structure but not covalent bonds (Sun et al., 2016; Guo et al., 2018). Based on the size/shape-fit of the guest molecules and the inner cavity of β-CD, guest molecules can bind into inner cavity of β-CD to form stable inclusion complex (Freeman et al., 2009; Rekharsky and Inoue, 1998). Owing to its stable host-guest interaction, great biocompatibility and good water solubility, β-CD has been widely applied in various electrochemical biosensors in recent years (Mukdasai et al., 2018; Kubendhiran et al., 2018).

In this paper, a new electrochemical aptasensor for the detection of AFB1 was designed based on the smart host-guest recognition between ferrocene (Fc) and β-CD. To improve the electron transfer property of the bare GC electrode, gold nanoparticles were deposited on the surface of the GC. Then, electrochemical polymerization of β-CD was carried out on the surface of the AuNPs/GC electrode by cyclic voltammetry. Without AFB1, ferrocene (Fc)-labeled probe DNA (Fc-cDNA) hybridized with Fc-labeled aptamer. Two ferrocene molecules were brought closely together and can't be recognized by β-CD. Once AFB1 captured the aptamer from the hybridization structure, Fc-cDNA were released and bound into β-CD. As a result, strong electrochemical signal were obtained. Thus, an inexpensive electrochemical aptasensor was successfully developed for simple and facile detection of AFB1 in real peanut oil by directly measuring the current or electron transfer resistance (R_{et}) changes.

2. Experiment section

2.1. Materials and reagents

Aflatoxin B1 (AFB1), Aflatoxin B2 (AFB2), ochratoxin A (OTA), fumonisin B1 (FB1), zearalenone (ZEN), deoxynivalenol (DON) were purchased from Pribolab Pte. Ltd (Singapore). Staphylococcal enterotoxin B (SEB) was purchased from Toxin Technology, Inc. (Sarasota, FL, USA). β-cyclodextrin (β-CD) and $HClO_4$ were obtained from Shanghai Reagent Company (Shanghai, China). Chloroauric acid ($HAuCl_4$) was purchased from Sinopharm Chemicals Reagent Co. Ltd (Shanghai, China). All other chemicals were of analytical reagent grade. All solutions were prepared using ultrapure water (18.2 MΩ cm at 25 °C) from a Milli-Q water purification system (Barnstead, Thermo Scientific, USA).

DNA hybridization buffer (H-buffer) contained 10 mM Tris-HCl, 0.1 M NaCl (pH 7.4). The reaction buffer (R-buffer) was composed of 0.1 M PB solution (pH 7.4, 0.1 M KCl). The cDNA and AFB1 aptamer were synthesized by Sangon Biotech Co. Ltd. (Shanghai, China). And the sequences were listed as follow:

AFB1 aptamer: 5′GT TGG GCA CGT GTT GTC TCT CTG TGT CTC GTG CCC TTC GCT AGG CCC ACA-Fc 3′
cDNA: 3′AGC GAT CCG GGT GT-Fc 5′

2.2. Instrumentation

All cyclic voltammetry (CV) and differential pulse voltammetry (DPV) spectra were conducted on a CHI 660D electrochemical analyzer (Chenhua Instruments, Shanghai, China). A conventional three-electrode cell was used with a saturated calomel electrode (SCE) as the reference electrode, a platinum wire as the counter electrode and glassy carbon electrode as the working electrode. AC impedance was achieved on Gamry Reference 600 potentiostat/galvanostat/ZRA (USA). All the electrochemical experiments were performed at room temperature.

2.3. Preparation of the pβ-CD/AuNPs/GC electrode

The modification of bare GC electrode was prepared according to the previously reported method (Li et al., 2017). In brief, the pretreated GC electrode was immersed in $HAuCl_4$ aqueous solution (2%) and kept at a constant potential of − 0.2 V for 60 s to electrodeposit gold nanoparticles (AuNPs) on the surface of GC electrode. The obtained electrode was washed with ultrapure water, allowed to dry in air and defined as AuNPs/GC electrode. Then, the AuNPs/GC electrode was immersed in 0.04 M β-CD/1 M $HClO_4$ aqueous solution. And electrochemical polymerization of β-CD was carried out on the surface of the AuNPs/GC electrode by cyclic voltammetry in the potential range from 0 to 1.3 V with a scan rate of 100 mV/s for 30 cycles under N_2 atmosphere. The prepared electrode was cleaned carefully with ultrapure water and named as pβ-CD/AuNPs/GC electrode. The mechanism of electropolymerization of β-CD is explained as follows. First, the primary carbon of β-CD is oxidized into aldehyde group or carboxyl group (Alarcon-Angeles et al., 2010). Next, the oxidized β-CD moleculars with aldehyde group or carboxyl group reacts with another β-CD molecular to form dimers. By repeating scanning, the degree of polymerization increased. And finally, the polymers are electropolymerized on the surface of electrode (Morales et al., 2003; Angeles et al., 2011). Finally, the pβ-CD/AuNPs/GC electrode was incubated with BSA solution (1%) for 60 min at 37 °C to avoid the nonspecific absorption.

2.4. Preparation of AFB1-sensitive dsDNA

According to the previous reports (Xu et al., 2017; Fan et al., 2016; Wu et al., 2018), 5 μL of Fc-cDNA (25 μM) and 5 μL of Fc-labeled AFB1 aptamer (25 μM) were mixed with 20 μL of H-buffer, followed by heating to 95 °C for 5 min and then naturally cooling down to room temperature for 2 h. Then AFB1-sensitive dsDNA was obtained.

2.5. Determination of AFB1 by electrochemical measurements

60 μL of different concentrations of AFB1 diluted by R-buffer was incubated with AFB1-sensitive dsDNA solution for 60 mins at 37 °C. Strong affinity between AFB1 and aptamer made Fc-cDNA release from the AFB1-sensitive dsDNA. Then 10 μL of mixture solution was dropped on the surface of the pβ-CD/AuNPs/GCE for 60 min incubation. Fc-cDNA was assembled on the electrode based on the unique host-guest interaction between β-CD and Fc. Then, the electrode was rinsed thoroughly with 10 mM PB solution (pH 7.4) and dried with a stream of nitrogen. Finally, the electrode was immersed in 0.1 M PB solution (pH 7.4, 0.1 M KCl) for the DPV detection with a fixed pulse amplitude of 0.05 V. For the AC impedance intensity measurement, the prepared Fc-cDNA/pβ-CD/AuNPs/GC electrodes were also immersed in 0.1 M KCl aqueous solution containing 5 mM K_3 $[Fe(CN)_6]$/$K_4[Fe(CN)_6]$. And the impedance spectra were recorded in the range of 0.1 Hz–100 kHz with AC amplitude of 5 mV.

3. Results and discussion

3.1. Principle of electrochemical sensing strategy

Detailed mechanism for the quantitative detection of AFB1 based on smart host-guest recognition is illustrated in Scheme 1. The AFB1-sensitive dsDNA was designed as the probe which was benefited from the tendency of AFB1 aptamer to form a duplex structure with its complementary cDNA. The principle of the size and shape matching was the most essential factor to influence the host-guest interaction. According to the result of DFT calculations (Jiang et al., 2017), the length and width of ferrocene were 4.4 Å and 3.5 Å, respectively (Fig. 1A). The internal diameter of β-cyclodextrin cavity was about 6.0–6.5 Å (Fig. 1B). So, only one ferrocene molecule could enter into the β-cyclodextrin cavity to form inclusion complexes based on the hydrophobic

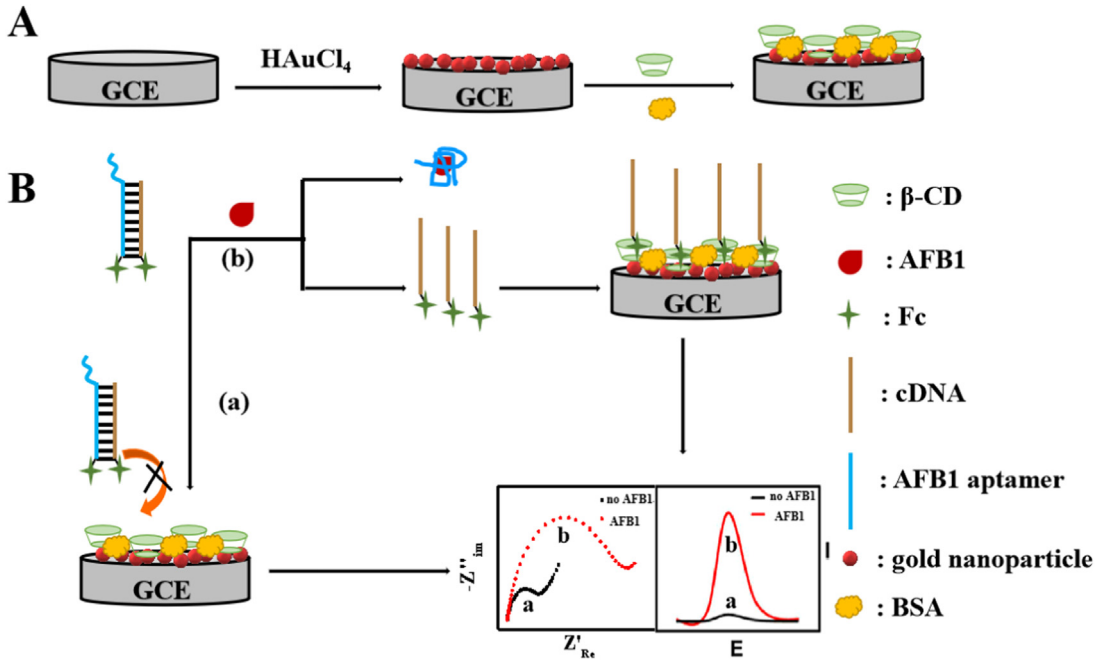

Scheme 1. Schematic illustration of the fabrication of the electrochemical aptasensor for AFB1 and its detection strategy.

interaction between internal group of β-CD and Fc. However, two paratactic ferrocene molecules could not enter into the cavity of β-CD because of their unmatched size.

In the absence of AFB1, the dimension of paratactic ferrocene labeled on AFB1-sensitive dsDNA was too large to enter into the cavity of β-CD (route a). Weak current response and R_{et} value was observed (curve a). In the presence of AFB1, the AFB1 aptamer was captured from the hybridization structure due to the higher affinity of the aptamer to the target (AFB1). Fc-cDNA was released and captured by β-CD polymerized on the electrode (route b). As a result, current and R_{et} increased obviously, which depended on the amount of captured Fc-DNA (curve b). Therefore, the electrochemical aptasensor has prospect to be used for AFB1 detection.

3.2. Characterization of the preparation of pβ-CD/AuNPs/GC electrode

The morphology of the bare GC, AuNPs/GC and pβ-CD/AuNPs/GC had been investigated by SEM. Before modification, nothing could be observed on the bare GC electrode (Fig. 2A). After the electrodeposited of Au on the GC electrode, a layer of homogeneous AuNPs was formed on the surface of GC electrode (Fig. 2B). It was clear that AuNPs on the GC electrode provided a large surface area for the electropolymerization of pβ-CD. The inset was the detailed porphology of the AuNPs. The function of AuNPs on the polymerization of β-CD and the detection performance is showed in Fig. S1. As is shown in Fig. 2C, the surface of the pβ-CD/AuNPs/GC electrode was much different from that of the AuNPs/GC electrode. Well-distributed film was observed on AuNPs/GC electrode, indicating the successful electropolymerization of pβ-CD.

It is well known that electrochemical impedance spectroscopy (EIS) is one of the most powerful tools to study the interfacial properties of electrodes. It was also applied to evaluate the stepwise fabrication of electrode by using $[Fe(CN)_6]^{3-/4-}$ as redox probe (Xiong et al., 2015; Zhu et al., 2015). The value of the diameter of the semicircle reflects the interfacial charge-transfer resistance (R_{et}), which is the most directive and sensitive parameter in response to the changes at the electrode/solution interface (Deng et al., 2009; Bardea et al., 1999). As is shown in Fig. 3A, the bare GC electrode showed a small semicircle domain (R_{et} = 202.1 Ω, curve a), implying a fast charge-transfer process. After coated with AuNPs, the R_{et} value decreased obviously (R_{et} = 77.2 Ω, curve b), suggesting that the electron transfer ability of the GC

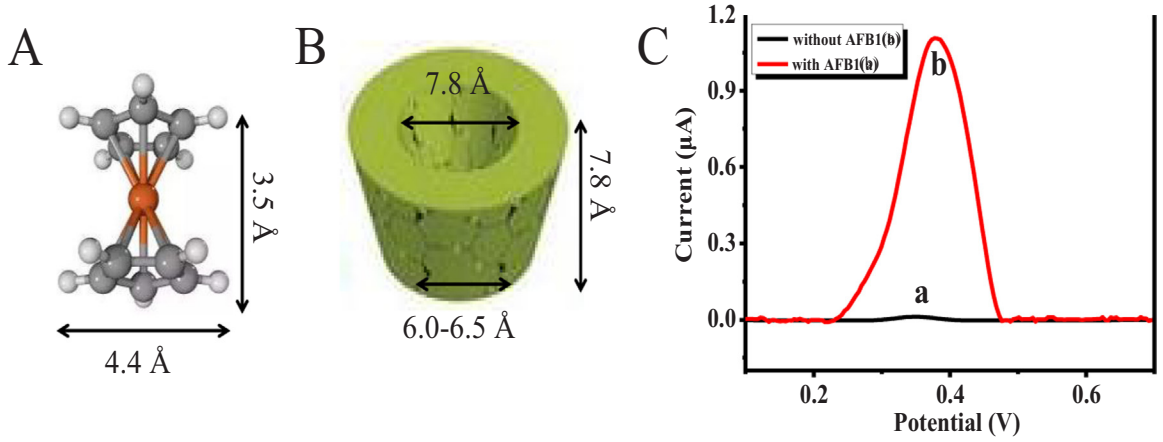

Fig. 1. (A) The molecular model of Fc and calculated dimensions. (B) The cavity diameter of β-cyclodextrin. (C) DPV curves of the pβ-CD/AuNPs/GC electrodes incubated with and without AFB1 (100 nM) in the same condition.

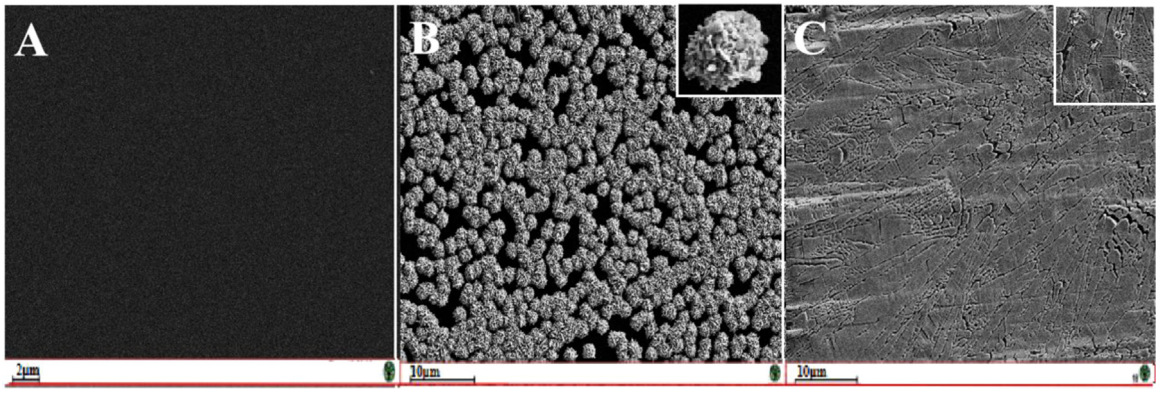

Fig. 2. SEM images of (A) GC, (B) AuNPs/GC and (C) pβ-CD/AuNPs/GC electrodes.

electrode was enhanced due to the excellent electrochemical properties of AuNPs. Due to the poor electronic conductivity of β-CD, the electropolymerization of β-CD film on the GC electrode blocked the electron transfer of $[Fe(CN)_6]^{3-/4-}$ on the electrode, resulting in an increment R_{ct} of 106.7 Ω (curve c). When Fc-cDNA was introduced to the electrode based on the host-guest recognition, R_{et} value increased obviously (4160.5 Ω, curve d). These results certified each step of modification on the electrode.

The modification processes of the Fc-cDNA/pβ-CD/AuNPs/GC electrode were also characterized by cyclic voltammetry (CV). Fig. 3B showed the well-defined redox peak of $[Fe(CN)_6]^{3-/4-}$ were observed at the GC electrode (curve a). When the electrode was modified with AuNPs film, the corresponding redox peak currents increased obviously, suggesting that AuNPs could promote the electron transfer (curve b). After electropolymerization of pβ-CD on the AuNPs/GC electrode, the peak current decreased due to the poor electronic conductivity of pβ-CD film (curve c). Upon the successful formation of an inclusion complex between Fc and β-CD, both of the oxidation peak and reduction peak of $[Fe(CN)_6]^{3-/4-}$showed obvious shift (curve d). These results also demonstrated that the Fc-cDNA/pβ-CD/AuNPs/GC electrode had been fabricated successfully.

3.3. Optimization of reaction conditions

The detection sensitivity of the proposed electrochemical aptasensor was influenced by the detection conditions. In order to optimize the key parameters, a series of experiments were done to test the influence of incubation time, reaction temperature and electropolymerization cycle number of β-CD on the detection of AFB1. Fig. S2A showed that the value of current leveled off in the 60 min with the increasing time, therefore, 60 min was selected as the best incubation time for AFB1 and AFB1-sensitive dsDNA. As is shown in Fig. S2B, From 15 to 37 °C, the value of peak current increased sharply, while it decreased when the temperature is higher than 37 °C. Thus, 37 °C was selected as the optimal reaction temperature to examine the response of the electrochemical aptasensor. Fig. S2C showed the influence of electropolymerization cycle number of β-CD on the response peak current obtained on the pβ-CD/AuNPs/GC electrode. The current value increased with the increase of electropolymerization cycle number of β-CD. When the cycle number was 30, it reached a plateau and then decreased. In order to ensure the sufficient amounts of β-CD on the surface of AuNPs/GC electrode, the electropolymerization cycle number of β-CD was chosen as 30 in the following assays of AFB1. All of the parameters made the probe an excellent candidate designed for biological applications.

3.4. Analytical performance of the proposed electrochemical aptasensor for AFB1 detection

For the purpose of investigating the sensitivity of the designed aptasensor, different concentrations of AFB1 (0.1 pg/mL–10 ng/mL) were measured under the above optimized experimental conditions. As is

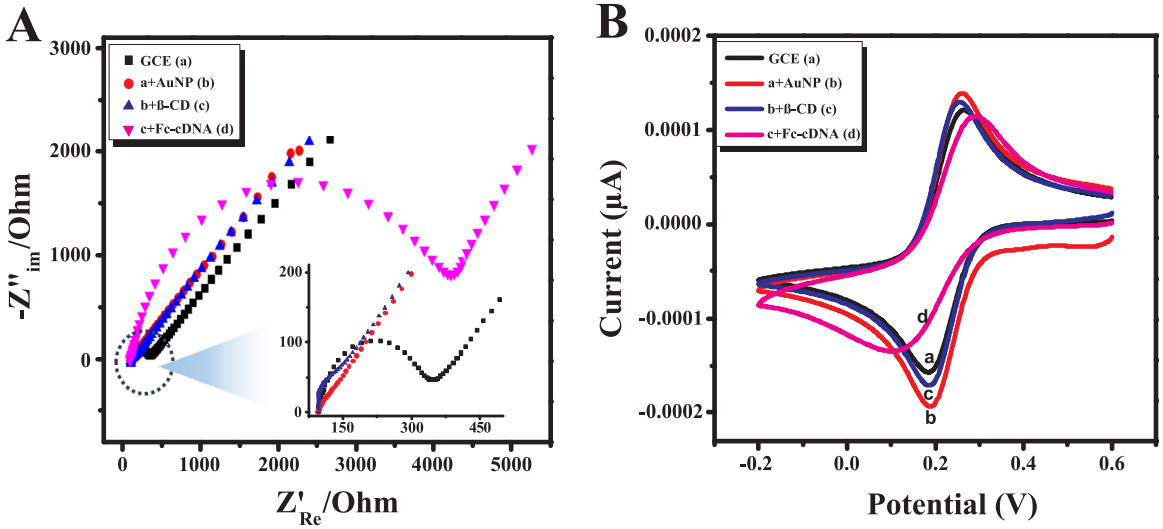

Fig. 3. (A) Nyquist plots recorded at (a) bare GC, (b) AuNPs/GC, (c) pβ-CD/AuNPs/GC, (d) Fc-cDNA/pβ-CD/AuNPs/GC electrodes in 0.1 M KCl aqueous solution containing 5 mM $K_3[Fe(CN)_6]/K_4[Fe(CN)_6]$. (B) Cyclic voltammograms of (a) bare GC, (b) AuNPs/GC, (c) pβ-CD/AuNPs/GC, (d) Fc-cDNA/pβ-CD/AuNPs/GC electrodes in 5 mM $[Fe(CN)_6]^{3-/4-}$ solution. Scan rate, 100 mV/s.

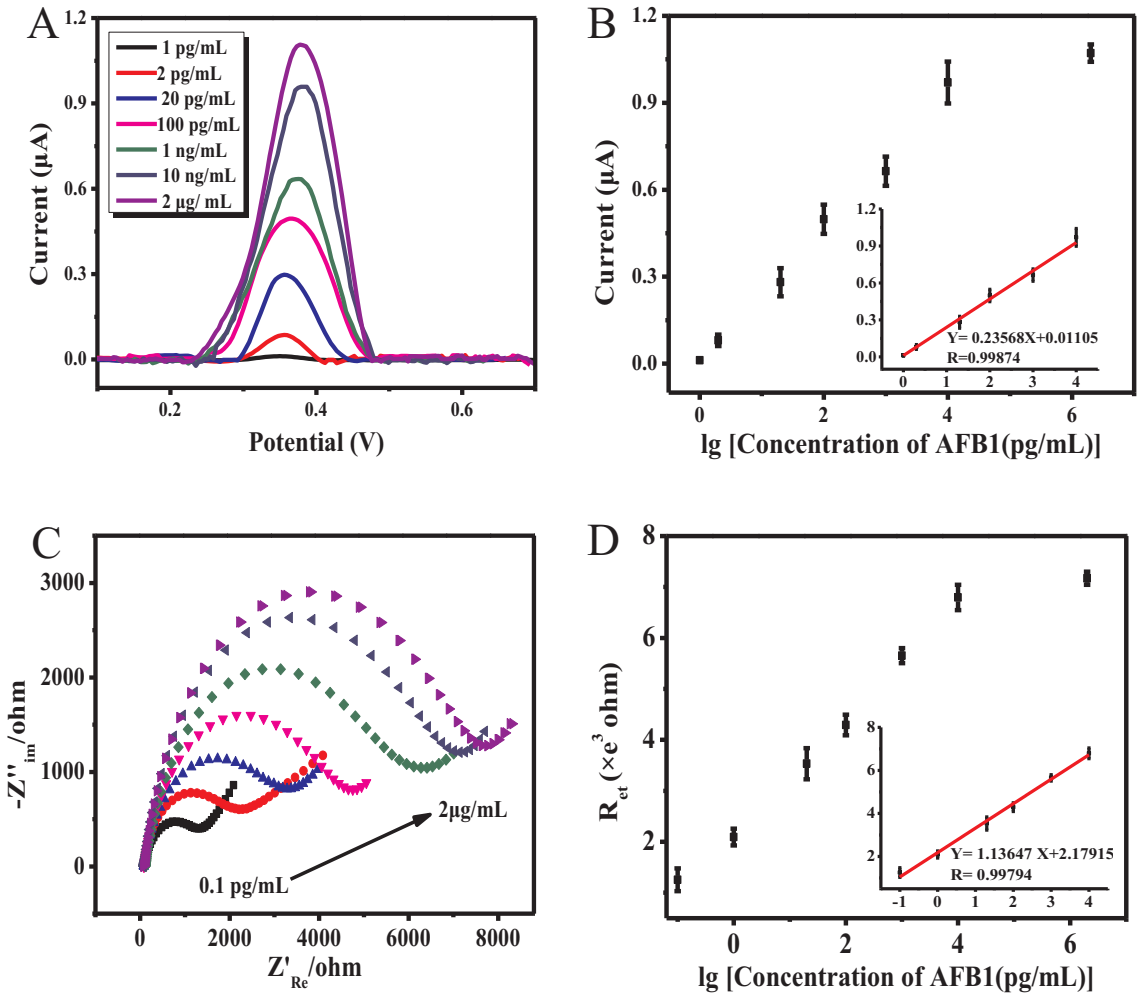

Fig. 4. (A) DPV responses of this proposed electrochemical aptasensor incubated with different concentrations of AFB1 and (B) calibration curve corresponding to the electrochemical intensity as a function of the logarithm concentration of AFB1. (C) Nyquist plots recorded at the pβ-CD/AuNPs/GC electrodes with different concentrations of AFB1 and (D) calibration curve corresponding to the value of R_{et} (the diameter of the semicircle) as a function of the logarithm concentration of AFB1. Results are shown as mean signals ± the standard error of the mean (n = 3).

shown in Fig. 4A, the peak value at 0.35 V in DPV increased with the increasing AFB1 concentration. A strong correlation between the electrochemical signal and the logarithm of AFB1 concentration (lg C_{AFB1}) ranging from 1 pg/mL to 10 ng/mL was obtained. The linear regression equation was expressed as Y = 0.23568x + 0.01105, R = 0.99874 (Fig. 4B). AFB1 activity down to 0.511 pg/mL (1.533 pmol/mL) could be calculated according to Fig. 4B (LOD = 3σ, σ means standard deviation of blank).

Furthermore, the quantitative detection was also detected by AC impedance. Compared with DPV, AC impedance had a broader linear range and lower LOD in AFB1 detection. A linear relationship between the value of the R_{et} (diameter of the semicircle) and the logarithm of AFB1 concentration (lg C_{AFB1}) was found in the range of 0.1 pg/mL–10 ng/mL (Fig. 4C). The correlation equation was Y = 1.13647x + 2.17915 (R = 0.9979). The detection limit, three times of standard deviation of blank, was calculated to be 0.0491 pg/mL (0.1473 pmol/mL) (Fig. 4D). Therefore, the following detection was conducted by AC impedance. Table S1 summarized a comparison of the analytical performances of other previous methods for the detection of AFB1. As a result, the calculated detection limit is about 10–100 times lower and the linear range is wider than most of them when AC impedance detection was used.

3.5. Selectivity, stability and reproducibility of the electrochemical aptasensor

The specificity of the aptasensor was further demonstrated by using other kinds of toxins including AFB2/AFB1, AFB2, FB1, DON, ZEA, SEB and OTA as control. As is shown in Fig. S3A, the presence of the other kinds of toxins led to negligible enhancement in the value of R_{et} compared to AFB1 at the same conditions. Therefore, the proposed electrochemical aptasensor exhibited good selectivity in discriminating AFB1 and other toxins.

What's more, we further tested the stability of the aptasensor. The long-term stability of the aptasensor was evaluated by storing the Fc-cDNA/pβ-CD/AuNPs/GC electrode at 4 °C and measuring the values of R_{et} at different times (1 day, 2 days, 5 days, 10 days, 15 days) under the same conditions (Fig. S3B). The values of R_{et} had no obvious difference and the relative standard deviations were less than 6.8%, suggesting that the proposed aptasensor had a satisfying stability for AFB1 detection. Reproducibility of the electrode was tested by regenerating the electrode 6 times for the same concentration of AFB1, results showed that the relative standard deviations were lower than 5.3%.

3.6. Detection of AFB1 in real peanut oil samples by the proposed method

To investigate the potential application of the electrochemistry

Table 1
Detection of AFB1 in real peanut oil samples by the proposed methods.

Sample	Concentration of AFB1(pg/mL)	Found	Recovery(%)	RSD(%,n = 3)
1	0.2	0.19	95.0	6.63
2	1.5	1.60	106.7	4.07
3	10	9.68	96.8	8.89
4	100	94.50	94.5	10.80
5	10000	10085.67	100.9	11.51

strategy in food safety, the developed electrochemical aptasensor was applied to detect AFB1 in real peanut oil samples. We spiked AFB1 standards with different concentrations (0.2, 1.5, 10, 100, 10000 pg/mL into blank peanut oil (diluted in 1:10 ratio with the reaction buffer). Results are summarized in Table 1. As shown in the table, the recoveries of the spiked samples ranged from 94.5% to 106.7%, with an inter-assay RSD lower than 11.51%, thus further indicating that the proposed aptasensor can be used for AFB1 detection in foodstuff with the satisfied results.

4. Conclusions

In summary, a simple electrochemical aptasensor based on the host-guest recognition between Fc and β-CD has been developed for sensitive determination of AFB1 by both DPV and AC impedance. The proposed aptasensor exhibited excellent performances in low detection limits and wide linear ranges. Although the proposed electrode can not be re-generated, it has good reproducibility and is highly sensitive and easy-operated when compared with the previously reported aptasensor. This strategy could also be applied to fabricate other aptasensors for various targets detection by replacing the corresponding aptamer.

CRediT authorship contribution statement

Shuang Shuang Wu: Data curation, Writing - original draft. **Min Wei:** Conceptualization, Methodology, Writing - review & editing. **Wei Wei:** Funding acquisition, Project administration, Writing - review & editing. **Yong Liu:** Formal analysis, Software. **Songqin Liu:** Supervision.

Acknowledgements

We gratefully appreciate the support from The National Key Research and Development Program of China (No, 2018YFC1602800), National Natural Science Foundation of China (21775019), Fundamental Research Funds for the Central Universities and A Project Funded by the Priority Academic Program Development of Jiangsu Higher Education Institutions (Grant Nos. 2242018K3DN04), The Open Project of The Key Laboratory of Modern Toxicology of Ministry of Education, Nanjing Medical University (NMUMT201804).

Notes

The authors declare no competing financial interest.

Declaration of interests

None.

Appendix A. Supplementary material

Supplementary data associated with this article can be found in the online version at doi:10.1016/j.bios.2019.01.022.

References

Angeles, G.A., Herrera, H., Corona-Avendano, S., Romero-Romo, M., Ramirez-Silva, M.T., Pardave, M.P., 2011. ECS Trans. 36, 439–446.
Alarcon-Angeles, G., Guix, M., Silva, W.C., Ramirez-Silva, M.T., Palomar-Pardave, M., Romero-Romo, M., Merkoci, A., 2010. Biosens. Bioelectron. 26, 1768–1773.
Annunziata, L., Stramenga, A., Visciano, P., Schirone, M., Colli, L.D., Colagrande, M.N., Campana, G., Scortichini, G., 2017. Anal. Bioanal. Chem. 409, 5143–5155.
Bardea, A., Patolsky, F., Dagan, A., Willner, I., 1999. Chem. Commun. 1, 21–22.
Deng, C., Chen, J., Nie, Z., Wang, M., Chu, X., Chen, X., Xiao, X., Lei, C., Yao, S., 2009. Anal. Chem. 81, 739–745.
Fan, J.H., Liu, Y.J., Xu, E.S., Zhang, Y.J., Wei, W., Yin, L.H., Pu, Y.P., 2016. Anal. Chim. Acta 946, 48–55.
Freeman, R., Finder, T., Bahshi, L., Willner, I., 2009. Nano Lett. 9, 2073–2076.
Gao, M.X., Guo, J.J., Song, Y.L., Zhu, Z., Yang, C.J., 2017. ACS Appl. Mater. Interfaces 9, 38356–38363.
Guo, F., Sun, Y., Xi, B., Diao, G., 2018. Supramol. Chem. 30, 81–92.
Hontanaya, C., Meca, G., Luciano, F.B., Mañes, J., Font, G., 2015. Food Control. 47, 154–160.
Irakli, M.N., Skend, A., Papageorgiou, M.D., 2017. J. Chromatogr. Sci. 55, 690–696.
Jiang, J.J., Lin, X.Y., Diao, G.W., 2017. ACS Appl. Mater. Interfaces 9, 36688–36694.
Knight, C.G., Platt, M., Rowe, W., Wedge, D.C., Khan, F., Day, P.J.R., McShea, A., Knowles, J., Kell, D.B., 2009. Nucleic Acids Res. 37, e6.
Kubendhiran, S., Sakthivel, R., Chen, S.M., Mutharani, B., Chen, T.W., 2018. Anal. Chem. 90, 6283–6291.
Li, X.Y., Li, J.J., Liu, Y.Q., Zhang, X.H., Chen, J.H., 2017. Sens. Actuators B: Chem. 250, 1–7.
Lin, Y.X., Zhou, Q., Tang, D.P., Niessner, R., Knopp, D., 2017. Anal. Chem. 89, 5637–5645.
Lin, Y., Zhou, Q., Lin, Y., Tang, D., Chen, G., Tang, D., 2015. Biosens. Bioelectron. 74, 680.
Ma, H., Sun, J., Zhang, Y., Bian, C., Xia, S., Zhen, T., 2016a. Biosens. Bioelectron. 80, 222–229.
Ma, H., Sun, J., Zhang, Y., Xia, S., 2016b. Biochem. Eng. J. 115, 38–46.
Mayne, L., Lin, C.Y., Christie, S.D.R., Siwy, Z.S., Platt, M., 2018. ACS Nano 12, 4844–4852.
Morales, G.R., Silva, T.R., Galicia, L., 2003. J. Solid State Electr. 7, 355–360.
Mukdasai, S., Poosittisak, S., Ngeontae, W., Srijaranai, S., 2018. Sens Actuators B Chem. 272, 518–525.
Platt, M., Rowe, W., Wedge, D.C., Kell, D.B., Knowles, J., Day, P.J.R., 2009. Anal. Biochem. 390, 203–205.
Reddy, K.R.N., Reddy, C.S., Muralidharan, K., 2009. Food Control. 20, 173–178.
Rekharsky, M.V., Inoue, Y., 1998. Chem. Rev. 98, 1875–1918.
Sun, Y., Ma, J., Tian, D., Li, H., 2016. Chem. Commun. 52, 4602–4612.
Wu, S.S., Wei, M., Yang, H.T., Fan, J.H., Wei, W., Zhang, Y.J., Liu, S.Q., 2018. Sens. Actuators B: Chem. 259 (5656-572).
Xia, N., Wang, X., Yu, J., Wu, Y., Cheng, S., Xing, Y., Liu, L., 2017. Sens. Actuators B: Chem. 239, 834–840.
Xiong, E., Zhang, X., Liu, Y., Zhou, J., Yu, P., Li, X., Chen, J., 2015. Anal. Chem. 87, 7291–7296.
Xu, L.L., Jiang, Z., Mu, Y.D., Zhang, Y.H., Zhan, Q., Cui, J., Cheng, W., Ding, S.J., 2018. Sens. Actuators B: Chem. 259, 596–603.
Xu, M., Gao, Z., Zhou, Q., Lin, Y., Lu, M., Tang, D., 2016. Biosens. Bioelectron. 86, 978–984.
Xu, X.L., Wei, M., Liu, Y.J., Liu, X., Wei, W., Zhang, Y.J., Liu, S.Q., 2017. Biosens. Bioelectron. 87, 600–606.
Zhao, Y., Huang, J., Ma, L., Wang, F., 2017a. Food Chem. 221, 11–17.
Zhao, Y.M., Houston, Zachary, H., Simpson, Joshua, D., Chen, L.Y., Fletcher, Nicholas, L., Fuchs, Adrian, V., Blakey, Idriss, Thurecht, Kristofer J.,, 2017b. Mol. Pharm. 14, 3539–3549.
Zhou, X., Wu, S., Liu, H., Wu, X., Zhang, Q., 2016. Sens. Actuators B: Chem. 226, 24–29.
Zhu, Z., Shi, L., Feng, H., Zhou, H., 2015. Bioelectrochemistry 101, 153–158.